

# Finite Element Modelling of Temperature Distribution and Residual Stress in Butt Welded Joints

Rakesh Kumar<sup>1,\*</sup> and Gurinder Singh Brar<sup>2</sup>

<sup>1</sup>(PhD Student, IKGPTU, Kapurthala) Department of Mechanical Engineering, North West Group of Institutions, Dhudike (Moga), Punjab, India

<sup>2</sup>Department of Mechanical Engineering, Guru Nanak Dev Engineering College, Ludhiana, Punjab, India

\*Corresponding Author- E-mail: [hod\\_me@northwest.ac.in](mailto:hod_me@northwest.ac.in)

## ABSTRACT

Welding is one of the most important assembling methods which are widely used in different applications. In the present work to predict residual stresses in the butt welded joint of two Fe<sub>3</sub> 410 WC steel plates, the thermo-mechanical three dimensional finite element analysis was performed by utilizing the MSC Marc-Mentat software. The simulation of welding process was done by using three dimensional finite element model and Goldak double ellipsoid heat source model. For the welding simulation, a sequentially coupled thermo-mechanical analysis was considered. The properties of the material depending upon temperature were specified. For the outward flux the heat losses of convective and radiations through boundary conditions were taken into account. The distribution of residual stresses and equivalent stresses are obtained in all directions. The welding process was simulated with nine different process parameter settings from the combination of welding process parameters and it was shown that by giving different heat inputs, there are variations in the temperature distribution and residual stresses. The maximum temperature and residual stresses were encountered when maximum heat input was supplied.

**Keywords:** Fe<sub>3</sub> 410 WC steel, Butt-welds, Finite element analysis, Welding residual stresses, Temperature distribution.

## I. INTRODUCTION

Welding is one of the most important method which is used to join different parts in almost all industries like ship, aircraft, automotive and bridge building etc. During the welding process, the internal stresses that exist in the structure and welded components are known as residual stresses which are induced by applying unequal temperature field. As the components/structure cool down to ambient temperature, the residual stresses develop which are associated with thermal cycles. The structural parameters (viz. welding geometry and type of welded joint), material properties (viz. physical and mechanical properties, and types of filler metal) etc. are strongly influence the distribution of residual stresses and welded joints distortion. The residual stresses are also affected by the welding process parameters (viz. welding current, welding voltage, travel speed of arc, arc efficiency and process used). The weld deformation,

fatigue, fracture, creep and buckling are strongly influenced by the results of these residual stresses.

Today still now welding processes have been considered as a weak point in the design of mechanical engineering in spite of the vast applications in the industry. The main reasons are due to the limitations in the welding technology, unfit of the mechanical properties and, last but not least, residual stresses in welding. Due to these, the analysis of these residual stresses in mechanical engineering design becomes an important task. The fatigue and creep lifetime also affected due to these residual stresses. These stresses not only reduce the lifetime of the weldment due to fatigue and creep but also produce undesirable deformation. As the highly localized tensile residual stresses which is well known produced due to welding that often approach the metallic yield stress but yet it is not completely know how residual stresses distributions are affected by these

various welding parameters. The counter measures against cracking and in service checking can be done with the help of this information. The final residual stresses are also affected by many factors, both related to the process and geometry dependent because of inherent complexities in the process of welding. The effect of welding residual stresses may either be advantageous or disadvantageous depending on the magnitude, nature (tension or compression) and the distribution of the stresses. Hence the mechanisms of metal deformation under both the internal and external conditions completely understand in which heat associated with the heat source of welding.

The prediction of distribution of these residual stresses in the welding process is very complicated and there is no analytical solution to calculate it due to highly nonlinear behavior. Hence, in the recent last decades numerical methods, especially finite element method in welding process analysis and simulation have become interesting to researchers. Study on the thermal stresses of welding process began in 1930 and the first solution was presented in 1936. In these years, for the first time computer was used to simulate the thermal stresses. Rosenthal [1] was among the first researcher that during welding developed an analytical solution of heat flow for determining the weld pool shape that was based on the conduction of heat for the modeling of two and three dimensional. He also introduced the system of moving coordinate to find the solutions for point and line modeling of the heat sources by using the equation of Fourier partial differential for the conduction of heat and a wide range of the modeling problems applied in a very successful way. Goldak et al. [2] on the basis of Gaussian distribution of power density derive a model for welding heat sources mathematically. In order to capture heat source size and shape of the shallow and deeper penetration they proposed the double ellipsoidal distribution. Tsai et al. [3] investigated effect on welding order on buckling and distortion of the thin plates. They also predicted the effect of welding parameters variation on both magnitude and distribution of the residual stresses in the thick plates. Duranton et al. [4] through multi-pass welding of a 316 L stainless steel by using 3D finite element simulations computed distortion and residual stresses. Murugan and Narayanan [5] in a T-joint for transient residual stresses performed finite element simulations of three dimensional and to

experimentally validate the numerical result used a contour method. Ueda and Yuan [6,7] and Mochizuki [8] to calculate the residual stresses used the inherent strain method. Stamenkovic and Vasovic [9] to predict residual stresses have performed a 3D finite element welding simulation in the butt welding of two carbon steel plates. The welding simulation was considered as a sequentially coupled thermo-mechanical analysis and for the simulation of filler metal deposition used the technique of birth and death of elements. A close relation was found between the finite element analysis results and experimental results. Tahami et al. [10] in butt welded 2.25 Cr1Mo steel plates the residual stress state has examined by the thickness effect. Finite element results show that there is increase in residual stresses and the zone of residual stress becomes larger by increasing the plate thickness. By increasing the plate thickness the welding residual stresses in the longitudinal axis changes from compressive to tensile. Tahami and Sorkhabi [11] studied the effect of welding electrode speed by using the birth and death of finite elements. Jeyakumar et al. [12] performed a 2D finite element analysis and predicted weld induced residual stresses in butt-welded of two similar 2.25 Cr1Mo low alloy ferritic steel and ASTM A36 steel plates. Murugan et al. [13] investigated residual stresses in AISI type 304 stainless steel and low Carbon steel V-groove pads of thickness 6, 8, 12mm welded by MMAW process. The peak residual stresses produced in stainless steel and low carbon steel was 193 MPa and 220 MPa found in the centre of weld bead. Tseng et al investigated the effect of pulsed GTA welding parameters on the welding residual stresses. The hole-drilling strain gage method was used to determine the residual stresses on the basis of ASTM standard E837. It was shown that the residual stress decreases in 304 stainless steel from 255 MPa to 200 MPa as the pulse frequency and pulse spacing increased. Chao et al [14] studied 304 L stainless steel plates by friction stir welding to show the transient temperature and residual stresses variations. It was also concluded that the longitudinal residual stress after fixture release decrease significantly as compared to those before fixture release by 470 MPa to 60 MPa as the increase in distance from weld centre. For analysis of welding thermal elastic plastic stresses and distortion some of the packages of finite element method (FEM) such as ABAQUS, ANSYS, NASTRAN, MARC etc. can be used which are commercially available. There are

many phenomenon involved for the simulation of welding residual stresses by the finite element are e.g material behavior dependent on temperature non linearly, 3D nature of weld pool and the welding processes and phase transformation due to changes in micro structure.

In this paper, the finite element simulation of residual stresses in butt welding of Fe<sub>3</sub> 410 WC low carbon steel plates is performed utilizing the MARC software. Fe<sub>3</sub> 410WC was selected as the material for the welding plates. This material has numerous applications in manufacturing the various structures and the parts such as bridges, steel structures, auto parts and industrial machines components. The 3D finite element model was investigated and the temperature distribution and residual stresses were obtained.

### The weld joint geometry and welding parameters

Two Fe<sub>3</sub> 410 WC steel plates with dimensions of 100 mm in length, 100 mm in width and 10 mm in thickness were butt-welded by the Metal Inert Gas (MIG) welding method using ER70S-6 electrodes. Figure 1 shows the schematic presentation of welding samples. The base metal chemical composition is shown in Table 1 and Welding parameters are shown in Table 2.

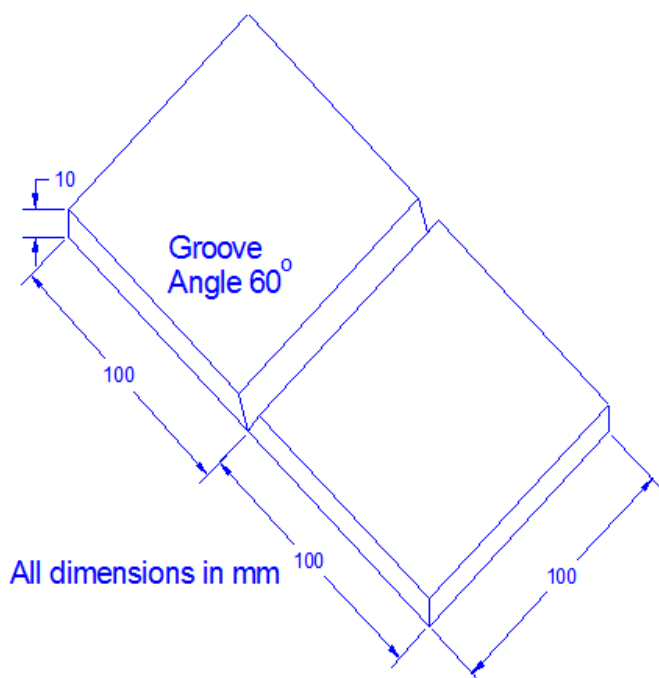


**Figure 1.** Schematic representation of welding samples

**Table 1.** Chemical composition of base metal (Wt %)

Grade	Fe	C	Mn	Si	P	Cr	Ni
Fe <sub>3</sub> 410 WC	Base	0.17	1.46	0.34	0.015	0.30	-

**Table 2.** Welding Parameters

Exp. Trial No.	Current (I) ampere	Voltage (U) volts	Welding speed V (cm/min.)
1	150	19	12.24
2	150	22	15.36
3	150	25	19.32
4	175	19	15.36
5	175	22	19.32
6	175	25	12.24
7	200	19	19.32
8	200	22	12.24
9	200	25	15.36

## II. METHODS AND MATERIAL

### Thermo-Mechanical analysis

Thermal and mechanical fields impress welding process. Since heat that arises from plastic strain is insignificant, the thermal and mechanical analysis could be accomplished independently. So, modeling of the arc welding process may be divided into two steps: heat transfer and mechanical analysis. In both thermal and mechanical analysis temperature dependent the thermo-physical and mechanical properties of the base metal were used in the computations. The material properties of Fe<sub>3</sub> 410 WC steel plates as the function of temperature including thermal conductivity, specific heat, yield stress, elastic modulus, Poisson ratio and thermal expansion coefficient were shown in Table 3.

**Table 3.** Physical and Mechanical properties of Fe<sub>3</sub> 410 WC steel plates

S. No.	Properties	Units
1	Elastic modulus	1.9 e <sup>+011</sup> N/m <sup>2</sup>
2	Poisson ratio	0.29
3	Shear modulus	7.5 e <sup>+010</sup> N/m <sup>2</sup>
4	Mass density	8000 kg/m <sup>3</sup>
5	Tensile strength	517017000 N/m <sup>2</sup>
7	Yield strength	206807000 N/m <sup>2</sup>
8	Thermal expansion coefficient	1.8e <sup>-005</sup> / Kelvin
9	Thermal conductivity	16 w/m. K
10	Specific heat	500 J/ Kg. K

**a) Thermal analysis**

The thermal transfer of welding process is time-dependent problem. The heat conduction was assumed to be governed by Fourier law:

$$\rho c_p \frac{\partial T}{\partial t} = \frac{\partial}{\partial x} \left( k_x \frac{\partial T}{\partial x} \right) + \frac{\partial}{\partial y} \left( k_y \frac{\partial T}{\partial y} \right) + \frac{\partial}{\partial z} \left( k_z \frac{\partial T}{\partial z} \right) + q_v$$

In this equation denotes the density (kg/m<sup>3</sup>), c<sub>p</sub> is the pressure-constant specific heat (J/kg. K), T is the temperature (K), t is the time (s), k is the temperature dependent thermal conductivity(J/m .s/K), and q<sub>v</sub> is the rate of internal heat generation (W/m<sup>3</sup>.s). Two kinds of boundary condition including convection and radiation were considered in the thermal analysis. The surface convection according to the Newton law is given by:

$$q_{con} = h_{con} (T_s - T_{\infty})$$

Where h<sub>con</sub> is the film coefficient of convection (J/K.m<sup>2</sup>), T<sub>s</sub> is the surface temperature of plate (K) and T<sub>∞</sub> is the ambient temperature (K). It was assumed that the ambient temperature is 298K. Also heat loss due to radiation is another surface effect and according to the Stefan-Boltzmann law is given by:

$$q_{rad} = \epsilon \sigma (T_s^4 - T_{\infty}^4)$$

Where the surface emissivity is constant and is the Stefan-Boltzmann coefficient (J/K<sup>4</sup>.m<sup>2</sup>) Deng [15] represented the total temperature-dependent film coefficient by combining both convection and radiation effects as:

$$h = 0.68 \left( \frac{w}{m^2} \right) \text{ if } 0 < T < 500^{\circ} C$$

$$h = 0.231T - 82.1 \left( \frac{w}{m^2} \right) \text{ if } T > 500^{\circ} C$$

**Mechanical Analysis**

Innumerical analysis of welding to predict the residual stresses the thermal, elastic and plastic models are always necessary. Since phase transformation takes place at a relatively high temperature for the low carbon steel such as Fe<sub>3</sub> 410 WC, the change in volume and hence the transformation of phase can be ignored. Thus, the total strain is composed of an elastic, plastic and thermal part as:

$$\epsilon_{total} = \epsilon_e + \epsilon_p + \epsilon_t$$

Considering the equation, the constitutive equation may be expressed as follows:

$$\sigma = D = D(\epsilon_{total} - \epsilon_p - \epsilon_t)$$

Where D is the material stiffness matrix. The elastic – plastic behavior with the linear kinematic hardening was used as the material model. For typically low carbon steel Fe<sub>3</sub> 410WC, the yield stress considerably reduced with temperature rise and naturally vanished at the melting temperature.

**Finite Element Simulation**

The analysis for fusion welding is performed in two steps as an uncoupled problem. The transient thermal analysis is performed for the prediction of temperature distribution in the weldment. Later, mechanical analysis is performed under the so obtained thermal loads to get the evolution and distribution of residual stresses. The flow chart for the analysis procedure is given in Fig. 2. It is assumed that change in the thermal state cannot be affected by the change in mechanical state but change in

the mechanical state affected by the change in thermal state.

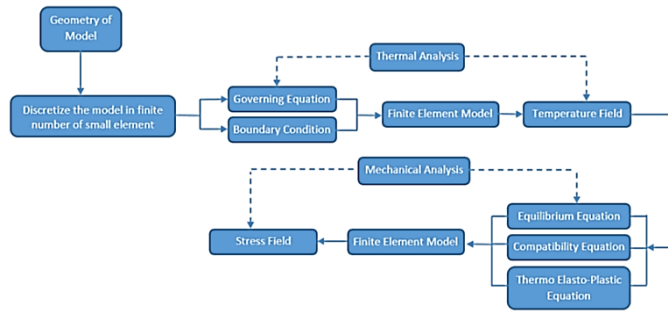


**Figure 2.** Flow chart of thermal and mechanical analysis.

#### 4.1 Finite Element Model:

In this research, for finite element modeling- MSC.Marc-Mentat software was applied to fulfill the thermal and mechanical analysis. Because of the symmetry of the welded plates only one of them was modeled. Figure 3 illustrates the mesh configuration of the welded plates in the thermal and mechanical analysis. Due to the presence of high temperature and the stress gradient near the weld line, a relatively fine mesh was provided and the element size was increased progressively with distance from the weld line. The simulation of the weld passes and deposition of filler metal into the weld pool was done by the element birth and death technique. In the finite element analysis 2340 eight node hexahedral elements are used to make the 3D meshing of the geometry for the thermal and mechanical analysis.

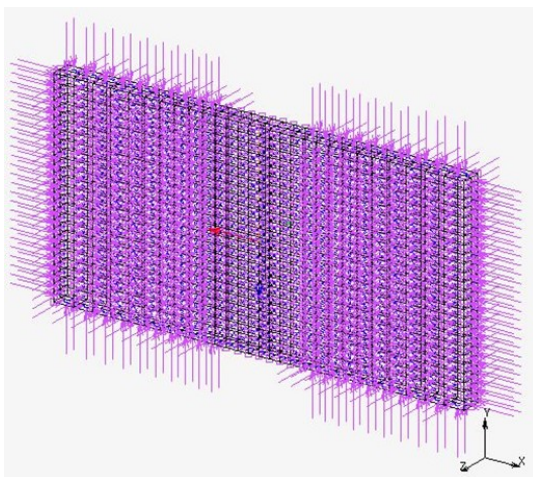


**Figure 3.** Finite element meshed model

The parameters that are used to model the thermal source resulting from electrical arc are the most important parameters to analyze the welding process.

These parameters are the zone of fusion (FZ), the zone of heat affected (HAZ) and the distribution of the heat input, the rate of cooling and thermal gradients. The heat input in welding or the electrical power of welding arc was calculated using the following equation:

$$Q = \eta VI$$

Where  $\eta$  is the arc efficiency,  $V$  is the voltage and  $I$  the current of the welding process.

To calculate the volumetric heat flux distribution a model was adopted which is known as Goldak double-ellipsoid heat source as the input heat into the pool of welding. The distribution of heat source shown in Figure 4 consists ellipses of two different categories i.e. one heat source in the front quadrant and other in the rear quadrant of it. The densities of power of the double ellipsoid heat source,  $q_f(x,y,z)$  and  $q_r(x,y,z)$  inside the front and rear quadrant of the heat source which describe the heat flux distribution can be expressed as [16]:

$$q_f = \frac{6\sqrt{3}Qf_f}{abc_f\pi\sqrt{\pi}} e^{-3\left(\frac{x^2}{a^2}\right)} e^{-3\left(\frac{y^2}{b^2}\right)} e^{-3\left(\frac{z^2}{c_f^2}\right)}$$

$$q_r = \frac{6\sqrt{3}Qf_r}{abc_r\pi\sqrt{\pi}} e^{-3\left(\frac{x^2}{a^2}\right)} e^{-3\left(\frac{y^2}{b^2}\right)} e^{-3\left(\frac{z^2}{c_r^2}\right)}$$

In the above equation, weld width  $a$  is along the tangent direction  $x$ ; depth of weld penetration  $b$  is along the arc direction  $y$ ; and the forward length  $C_f$  and rear weld pool length  $C_r$  in the weld path direction  $z$ ; and  $f_f$  and  $f_r$  are some dimensionless factors.

Two parameters  $C_f$  and  $C_r$  were determined using the following relationship [17]

$$c_f \in (0.5a, a) \ \& \ c_r \in (2a, 4a)$$

Two dimensionless factors  $f_f$  and  $f_r$  were obtained from the following equations [18]

$$f_f = \frac{2c_f}{c_f + c_r} \ \& \ f_r = \frac{2c_r}{c_f + c_r}$$

The parameters of the heat flux distribution were calculated using the above discussion and are shown in Table 4.

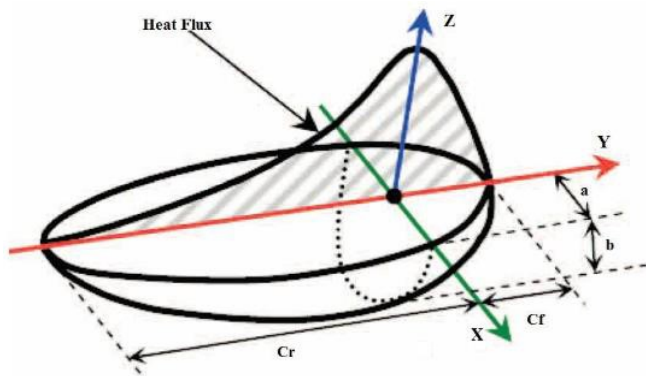


**Figure 4.** The Goldak double-ellipsoid heat source model

**Table 4.** The parameters of the heat flux distribution

Parameters	a	b	C <sub>f</sub>	C <sub>r</sub>	f <sub>f</sub>	f <sub>r</sub>
Value (mm)	2.5	3	2.5	7.5	0.5	1.5

The mechanical analysis was conducted based on the thermal analysis results. The nodal temperatures from the associated transient heat transfer analysis were the only applied loads to the stress analysis. Since the inertia has an insignificant effect on the mechanical properties of the plate, the static stress analysis was adopted in this study. In mechanical analysis to prevent the motion of rigid body boundary conditions are used. Because of the finite element model in symmetrical shape the symmetric plane is fixed in x-direction. The one edge was constrained in both x and z directions and the other edge were constrained only in y-direction. Also the parts of plates that were in contact with the fixture were constrained in y direction.

### III. Results of Finite Element Analysis

To determine the distribution of temperature in the welded component the input of heat is the most important parameter. To fabricate the welded joints the output is heat quantity which is achieved from a particular heat source. In all the welding processes, the localized high temperature spot are caused by the energy which is provided by the heat source. The input of heat

during welding is modeled in the MSC Marc-Mentat software by the equivalent heat input which includes heat flux of the body. The amount of input of heat was calculated as follows:

$$Q = \frac{\eta UI}{V}$$

Where:  $\eta$  is the efficiency of arc,  $V$  is the welding travel speed,  $U$  and  $I$  are the welding arc voltage and the welding current, respectively.

The residual stresses calculations in welding usually done on the temperature distribution basis and from the increment thermal strain  $\alpha\Delta T$  the thermal stress increment  $\Delta\sigma (=E\alpha\Delta T)$  is calculated. Here  $\alpha$  is the coefficient of thermal expansion and  $E$  is the modulus of elasticity. The residual stresses come not only from the shrinkage of welding but also from the quenching of surface (rapid cooling of the weld surface layers) and the transformation of phase (transformation of austenite during the cooling cycle).

The calculation starts with time  $t=0$  and for the initial temperature of the welded component the distribution of thermal stress is calculated. The thermal stress increment is added to the initial stress at step  $t=0$  at the next time step. At actual temperature the magnitude of the commutative thermal stress is limited to the material yield strength. It should be noted that at each step, the forces must be in equilibrium which is caused by the induced thermal stress. The procedure is repeated until the last step at which the thermal stress is that at ambient temperature, i.e., the residual stress. The value of welding parameters, distribution of temperature and residual stresses are shown in Table 5.

**Table 5.** Welding parameters, Temperature distribution and Residual stresses

Exp. Trial No.	Current (I) ampere	Voltage (U) volts	Welding speed V (cm/min.)	Heat Input (Watts)	Temp (K)	Residual stress (MPa)
1	150	19	12.24	197.91	556	585
2	150	22	15.36	182.61	520	544
3	150	25	19.32	164.98	422	432
4	175	19	15.36	184	542	569
5	175	22	19.32	169.38	493	513
6	175	25	12.24	303.8	609	646
7	200	19	19.32	167.18	462	478
8	200	22	12.24	305.5	654	697
9	200	25	15.36	276.69	578	610

This can also be shown on a bar chart as shown in Figure 6 and Figure 7.

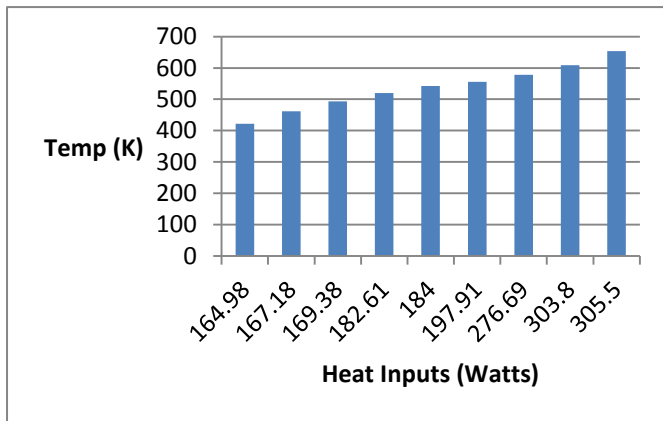


**Figure 6.** Bar chart between temperature distribution and heat input

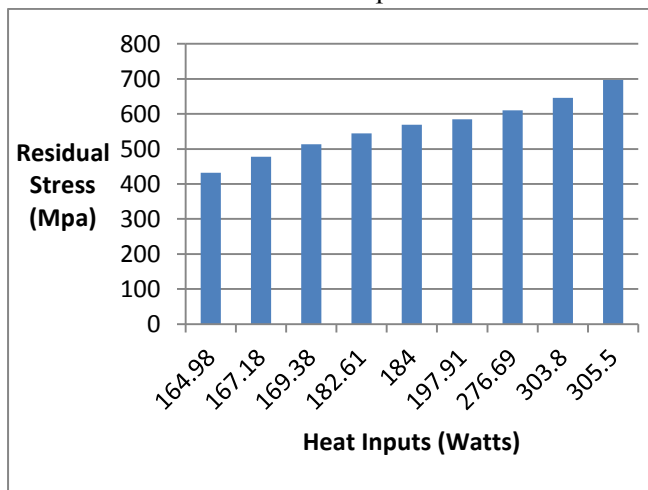


**Figure 7.** Bar chart between residual stresses and heat input

From the results of temperature distribution it is found that by giving the different heat inputs to the welding samples the temperature increases as the heat input increased e.g as the heat input supplied 164.98 watts, the temperature is 422° K and as we increase the heat input upto 305.5 watts, the temperature increases to a amount of 654° K. Similarly from the result of residual stresses it is found that as the heat supplied is 164.98° K, the value of residual stresses 432MPa and as we increases the heat input , the residual stress reaches up to a 697 MPa.

Figure 8 shows the residual stresses variations as the maximum heat input is supplied. It is shown that the residual stresses is maximum at the weld centre which is 697 MPa but as we move away from the centre of weld to the edge of the plates the residual stresses decreases suddenly which is 86 MPa that is known as the zone of

heat affected (HAZ) and the stress become normal after a certain distance.

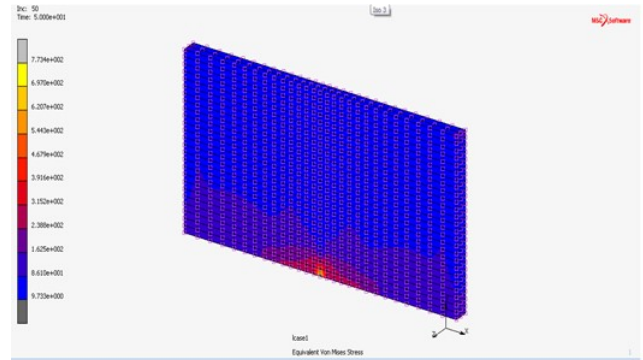
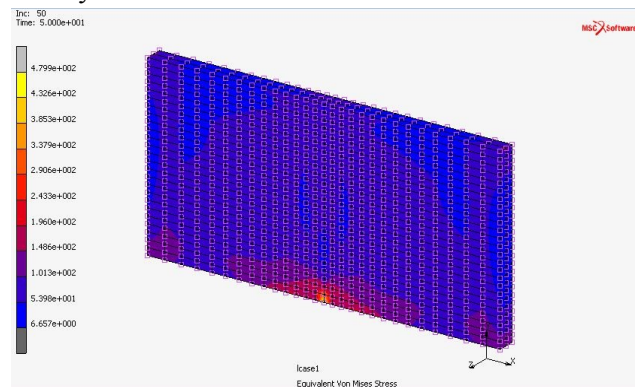


**Figure 8.** Variation of maximum residual stress with heat input

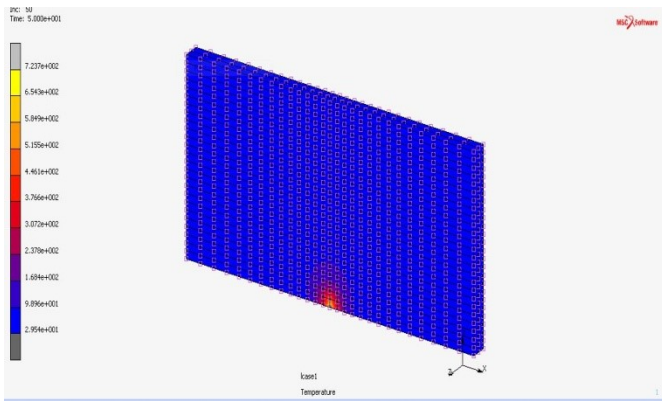
Figure 9 represent the variation of residual stress as the minimum heat input is supplied .It is shown that the residual stresses is maximum at the weld centre which is 432 MPa but as we move away from the weld centre to the edge of the plates the residual stresses decreases suddenly which is 53 MPa that is known as the heat affected zone (HAZ) and the stress become normal after a certain distance.

Figure 10 present the temperature variations as the maximum heat input is supplied .It is shown that the temperature is maximum at the weld centre which is 654° K but as we move away from the centre of weld to the edge of the plates the temperature decreases suddenly which is 98° K.

Figure 11 shows the variation of temperature as the minimum heat input is supplied .It is shown that the temperature is maximum at the weld centre which is 422° K but as we move away from the weld centre to the edge of the plates the temperature decreases suddenly which is 73° K.



**Figure 9.** Variation of minimum residual stress with heat input



**Figure 10.** Variation of maximum temperature with heat input

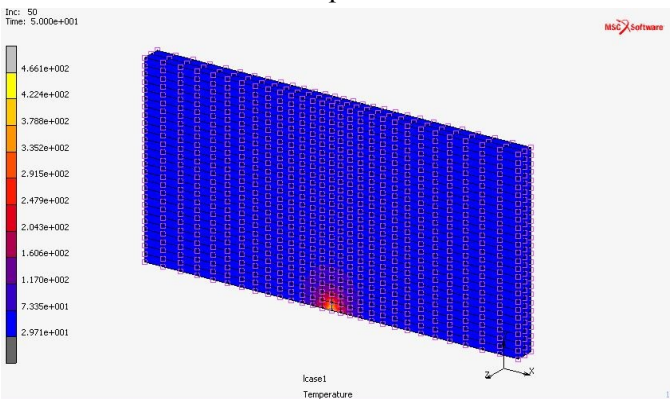


**Figure 11.** Variation of minimum temperature with heat input

Figure 12 shows the variation of Equivalent Von Mises Stress and at a distance of 25 mm from the weld centre line on both sides and it is found that the residual stresses is maximum at weld centre which is equal to 777.38 MPa but as we move away from weld centre to the edge of the plates the residual stress decreases suddenly which is known as heat affected zone (HAZ) and the stresses become normal after a certain distance.

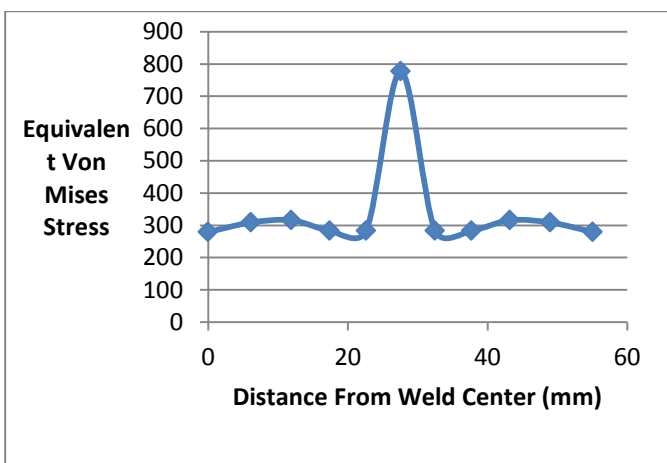
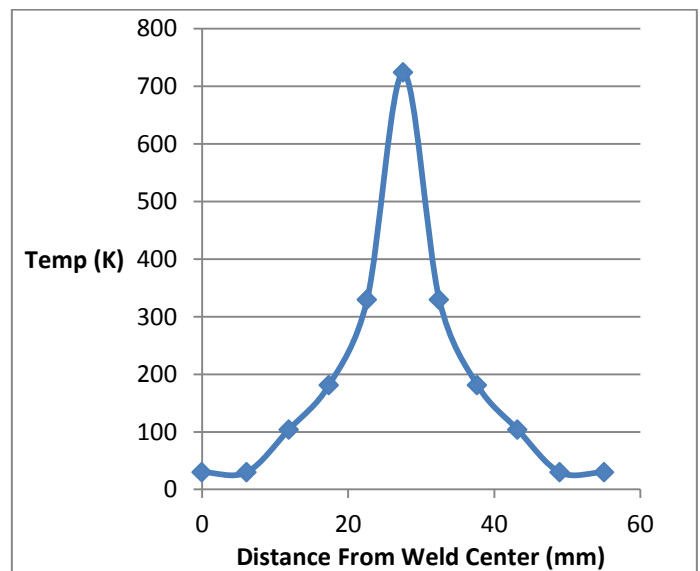


**Figure 12.** Variation of Maximum Equivalent Von Mises Stress with distance from weld centre line

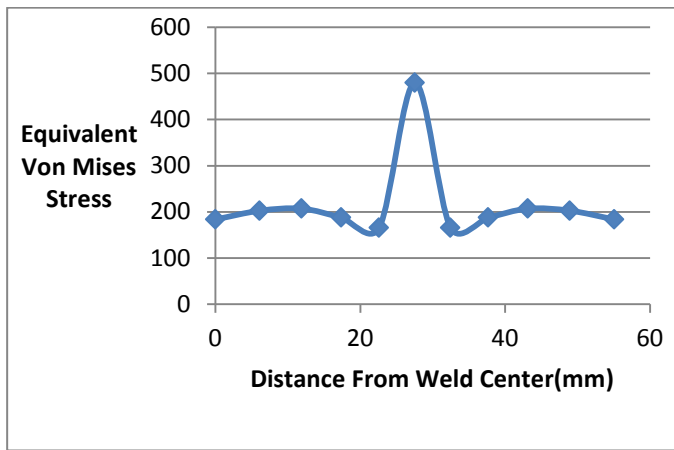
Figure 13 shows the Temperature variations and at a distance of 25 mm from the centre line of weld on both sides and it is found that the temperature is maximum at weld centre which is equal to 723.75K but as we move away from weld centre to the edge of the plates the temperature decreases suddenly which is known as heat affected zone (HAZ) and it become normal after a certain distance.

Figure 14 shows the variation of Equivalent Von Mises Stress and at a distance of 25 mm from the weld centre line on both sides and it is found that the residual stresses is maximum at weld centre which is equal to 479.89 MPa but as we move away from weld centre to the edge of the plates the residual stress decreases suddenly which is known as heat affected zone (HAZ) and the stresses become normal after a certain distance.

Figure 15 shows the variation of Temperature and at a distance of 25 mm from the weld centre line on both sides and it is found that the temperature is maximum at weld centre which is equal to 466.07K but as we move away from weld centre to the edge of the plates the temperature decreases suddenly which is known as heat affected zone (HAZ) and it become normal after a certain distance.



**Figure 13.** Variation of Maximum temperature with distance from weld centre line



**Figure 14.** Variation of Minimum Equivalent Von Misses Stress with distance from weld centre line

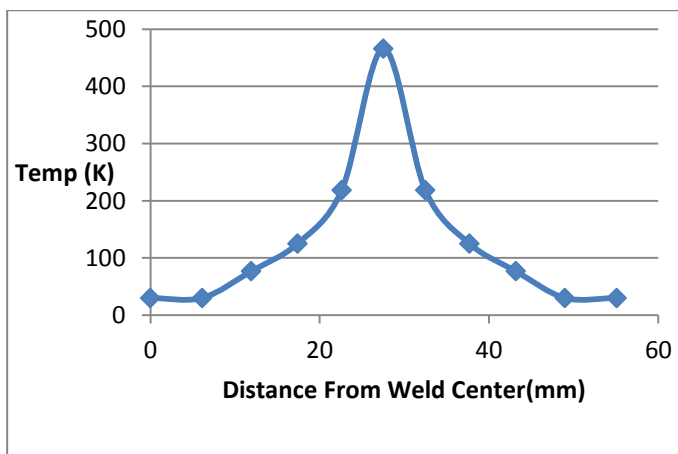


**Figure 15.** Variation of Minimum temperature with distance from weld centre line

#### IV. CONCLUSION

In the present work, numerical simulation of temperature distribution and residual stresses in welding by finite element analysis in Fe3 410 WC steel plates of butt welded joints was presented. For analyzing residual stresses in welding processes the finite element method is an efficient technique. A three-dimensional finite element welding simulation was carried out by MSC Marc-Mentat software with thickness of plates as 10 mm. A sequential coupled thermo-mechanical analysis was considered for the simulation of welding and for deposition of filler metal the technique of birth and death of finite elements was employed. The distributions of residual stresses by the analysis of finite element of two butt welded plates in the axial directions were presented. It can be concluded that by giving the different heat inputs to the welding samples the temperature increases as the heat input increased e.g as

the heat input supplied was 164.98 watts, the maximum temperature rose 422° K and as heat input was increased to 305.5 watts, the temperature increased to 654° K. Similarly from the result of residual stresses it is found that as more heat is supplied, the value of residual stresses increases from 432MPa to 697 MPa.

It can also be concluded that the magnitude of residual stress was maximum in the centre i.e. 777.38 MPa. Also the effect of residual stress is upto 25 mm distance on both sides of the weld centre which is known as heat affected zone (HAZ).

#### V. ACKNOWLEDGEMENT

Authors are highly thankful to the Department of RIC, IKG Punjab Technical University, Kapurthala, Punjab, India for providing the opportunity to carry out this research work.

#### VI. REFERENCES

- [1]. Rosenthal, D. (1941). Mathematical theory of heat distribution of welding and cutting. *Welding Journal*, Vol.20, No.5, pp.1007-16.
- [2]. Goldak, J., Chakravati, A. & Bibby, M. (1984). A new finite element model for welding heat sources. *Metallurgical Transactions B*, Vol.15B, pp. 299-305.
- [3]. Tsai, C.L., Park, S.C. & Cheng, W.T. (1999). Welding distortion of a thin-plate panel structure, *Welding Journal*, Vol.78, pp.156-65.
- [4]. Duranton, P., Devaux, J., Robin, V., Gilles, P. & Bergheau, J.M. (2004). 3D modeling of multipass welding of a 316L stainless steel pipe. *Journal of Material Process Technology*, Vol.153-154, pp. 457-463.
- [5]. Murugan, N. & Narayanan, R. (2009). Finite element simulation of residual stresses and their measurement by contour method. *Materials and Design*, Vol. 30, pp.2067-2071.
- [6]. Ueda, Y. & Yuan, M.G. (1993). Prediction of residual stresses in butt welded plates using inherent strains. *Transactions of the ASME, Journal of Engineering Materials and Technology*, Vol.115, No. 10, pp.417-423.
- [7]. Yuan, M.G. & Ueda, Y. (1996). Prediction of residual stresses in welded T- and I-joints using inherent strains. *Transactions of the ASME*,

- Journal of Engineering Materials and Technology, Vol.118, No.4, pp.229-234.
- [8]. Mochizuki, H. & Hattori, H. (1999). Residual stress analysis by simplified inherent strains at welded pipe junctions in a pressure vessel. Transactions of the ASME. Journal of Pressure Vessel Technology, Vol.121, pp.353-357
- [9]. Stemenkovic, D. & Vasovic, I. (2009). Finite element analysis of residual stress in butt welding two similar plates. Scientific Technical Reviews, Vol.59, No.59, pp.57-60.
- [10]. Tahami, F.V., Sorkhabi, A.H.D., Saeimis, M.A. & Homayounfar, A. (2009). 3D finite element analysis of the residual stresses in butt-welded plates with modeling of the electrode-movement. Journal of Zhejiang University Science A, Vol.10, pp.37-43.
- [11]. Tahami, F.V. & Sorkhabi, A.H.D. (2009). Finite element analysis of thickness effect on the residual stress in butt-welded 2.25Cr1Mo steel plates. Journal of Applied Sciences, Vol.9, pp.1331-1337.
- [12]. Jeyakumar, M., Christopher, T., Narayanan, R. & Rao, B.N. (2011). Residual stress evaluation in butt-welded steel plates, Indian Journal Engineering and Material Sciences, Vol.18, pp.425-434.
- [13]. Murugan, S., Rai, S.K., Kumar, P.V., Jayakumar, T., Raj, B. & Bose, M.S.C. (2001). Temperature distribution and residual stresses due to multipass welding in type 304 stainless steel and low carbon steel weld pads. International Journal of Pressure Vessels and Piping, Vol.78, Iss.4, pp.307-317.
- [14]. Zhu, X.K. & Chao Y.J. (2004). Numerical simulation of transient temperature and residual stresses in friction stir welding of 304L stainless steel, Journal of Materials Processing Technology, vol. 146, pp.263-272.
- [15]. Goldak, J., Chakravarti, A. & Bibby, M.J. (1984). A new finite element model for welding heat sources, Metallurgical Transactions B, Vol.15B, pp.299-305.
- [16]. Goldak, J.A. & Akhlaghi, M. (2005). Computational welding mechanics, Springer, New York.